Electronic Supplementary Material (ESI) for RSC Advances.
This journal is © The Royal Society of Chemistry 2016

Supporting Information For:

Synthesis and characterization of lipophilic cationic Ga(III) complexes based on the H_2*CHX*dedpa and H_2dedpa ligands and their $^{67/68}$Ga radiolabelling studies

C. F. Ramogida[1,2], D. Schindler[1], C. Schneider[1], Y. L. K. Tan[1], S. Huh[1], C. L. Ferreira[3], M. J. Adam[2], and C. Orvig[*,1]

[1]Medicinal Inorganic Chemistry Group, Department of Chemistry, University of British Columbia, 2036 Main Mall, Vancouver, British Columbia, Canada, V6T 1Z1. [2]TRIUMF, 4004 Wesbrook Mall, Vancouver, British Columbia, Canada, V6T 2A3. [3]Nordion, 4004 Wesbrook Mall, Vancouver, British Columbia, Canada, V6T 2A3.

*Corresponding author: orvig@chem.ubc.ca

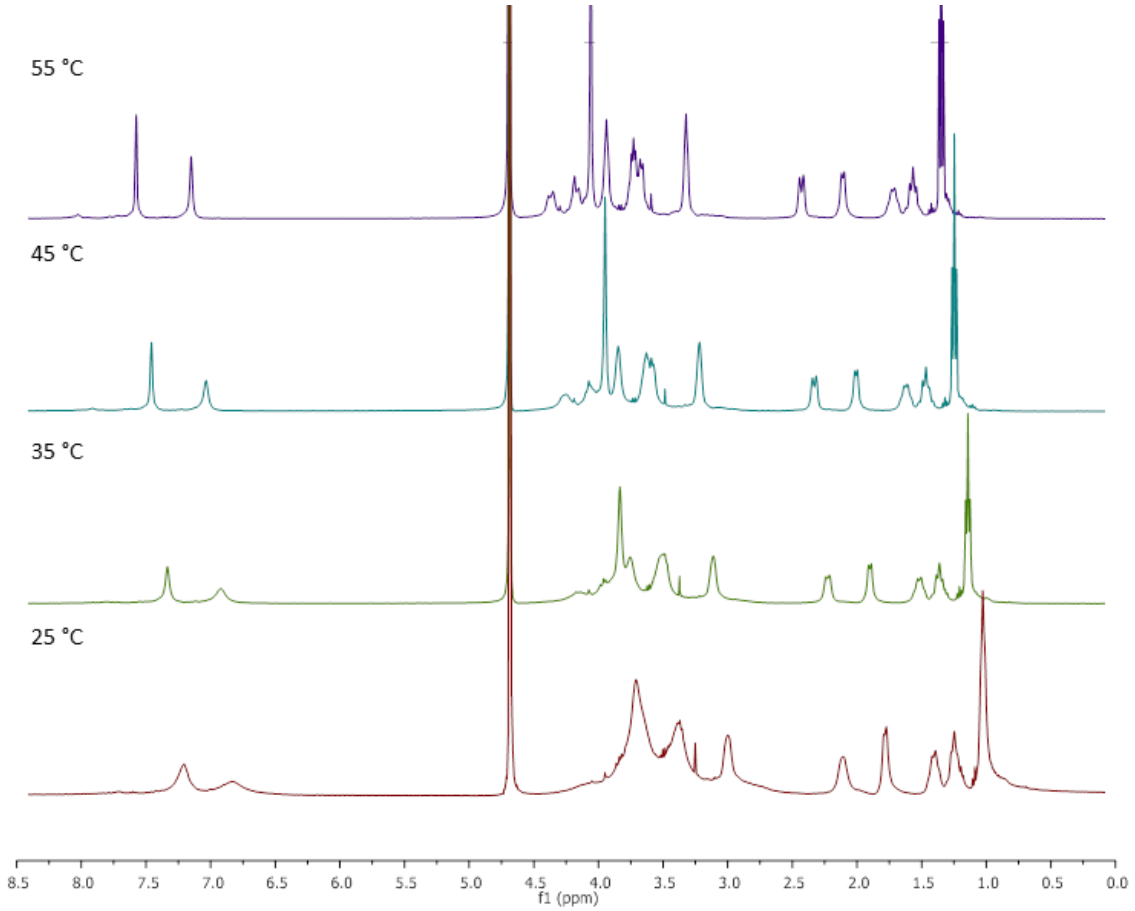

Figure S1. Variable temperature (VT) ^{1}H NMR spectra of H_2*CHX*dedpa$_{OMe}$-*N,N'*-ee (**12**) (400 MHz, D_2O, 25 – 55°C).

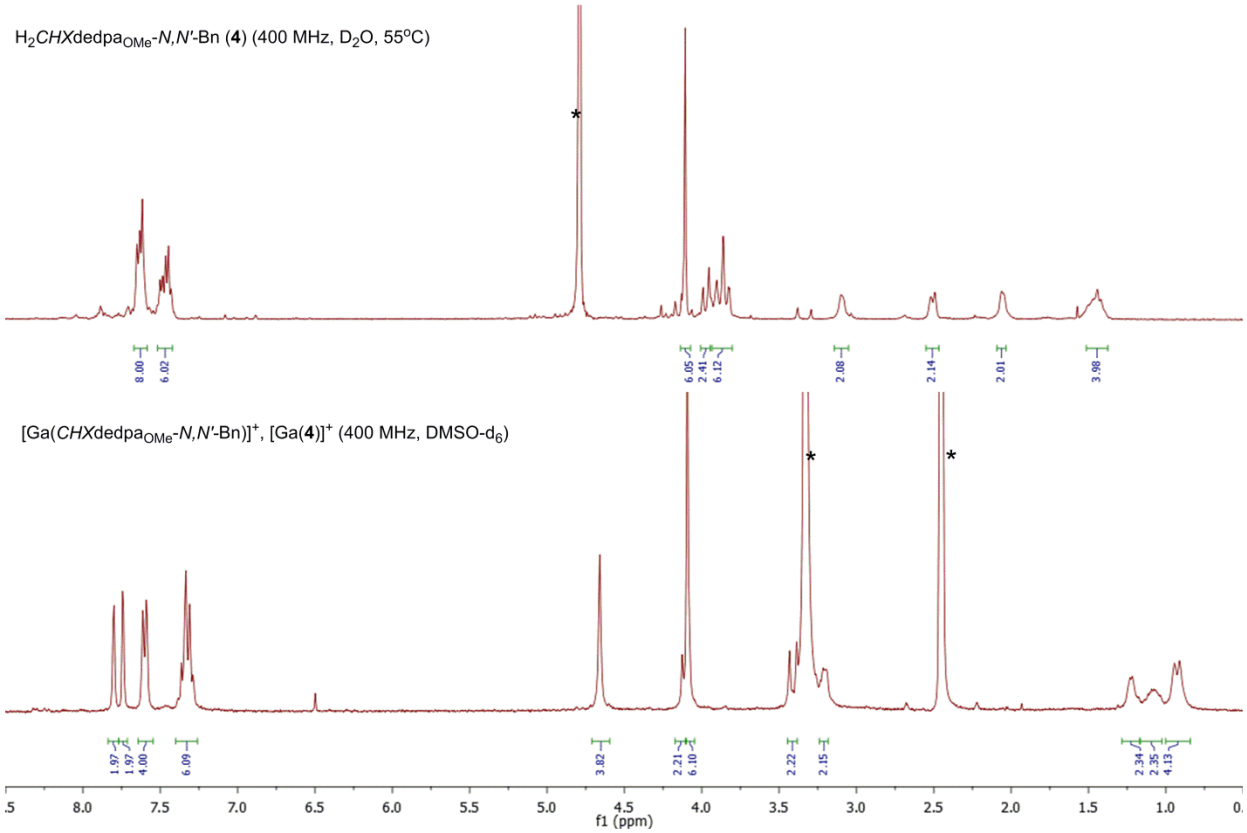

Figure S2. ^{1}H NMR spectra of (top) H_2dedpa$_{OMe}$-*N,N'*-Bn (**4**), 400 MHz, D_2O, 25°C) and (bottom) [Ga(**4**)]$^{+}$ (400 MHz, DMSO-d_6, 25°C), highlighting shifts in hydrogen resonances upon metal-complexation. *Residual solvent peak.

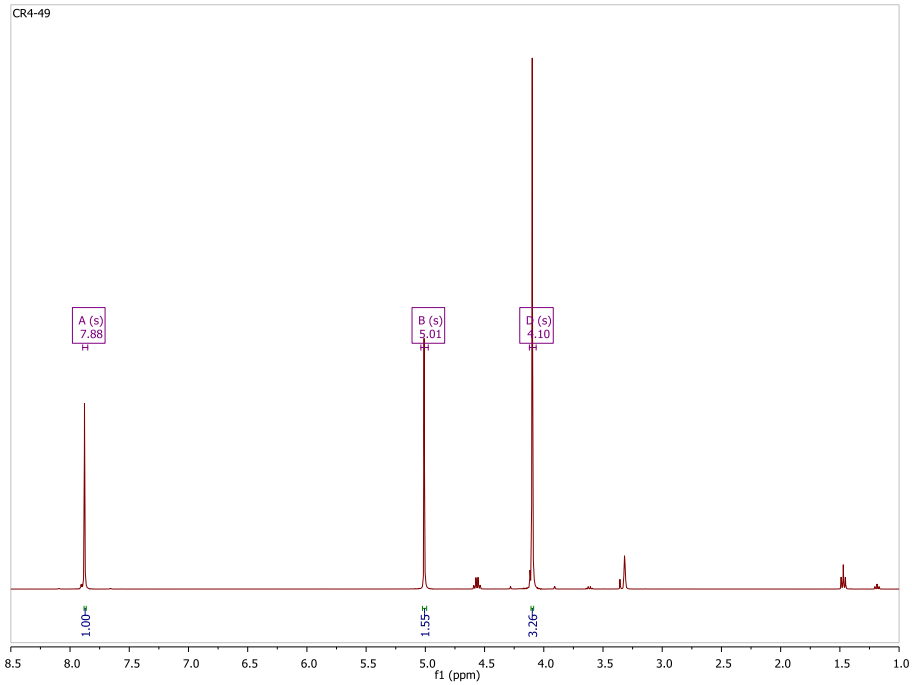

Figure S3. ^{1}H NMR of spectrum of dimethyl 4-hydroxypyridine-2,6-dicarboxylate (**7**) in MeOD-d_4 (400 MHz).

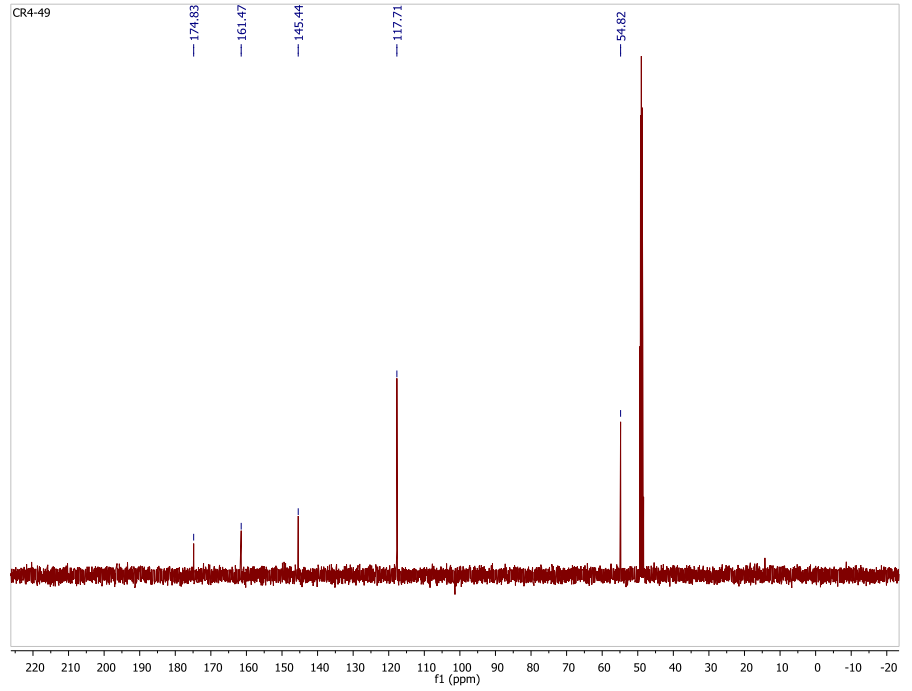

Figure S4. ^{13}C NMR of spectrum of dimethyl 4-hydroxypyridine-2,6-dicarboxylate (**7**) in MeOD-d_4 (101 MHz).

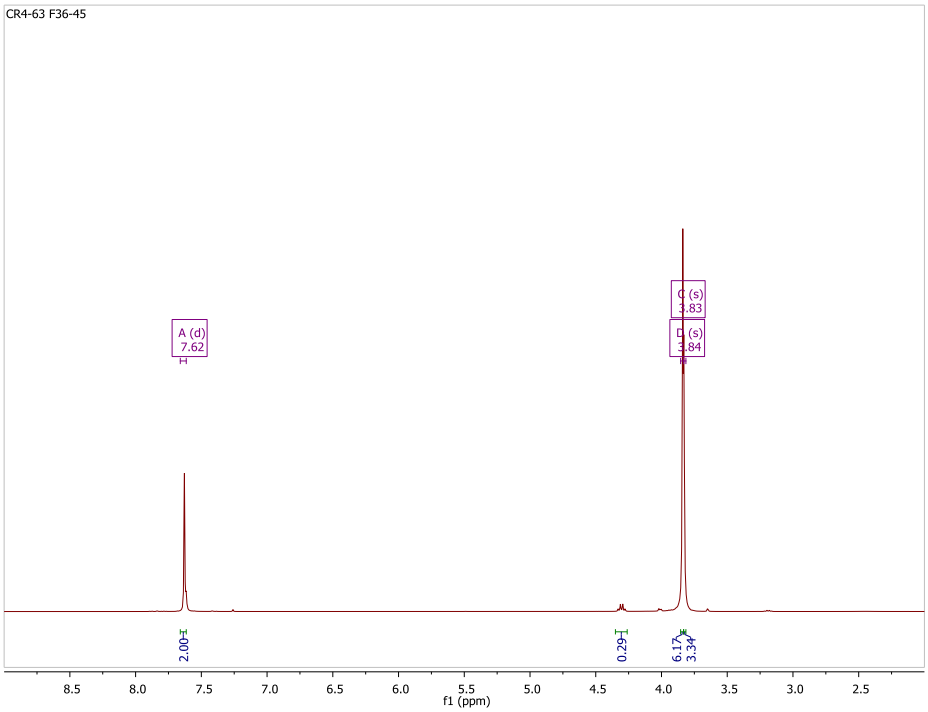

Figure S5. ^{1}H NMR of spectrum of dimethyl 4-methoxypyridine-2,6-dicarboxylate (**8**) in $CDCl_3$ (400 MHz).

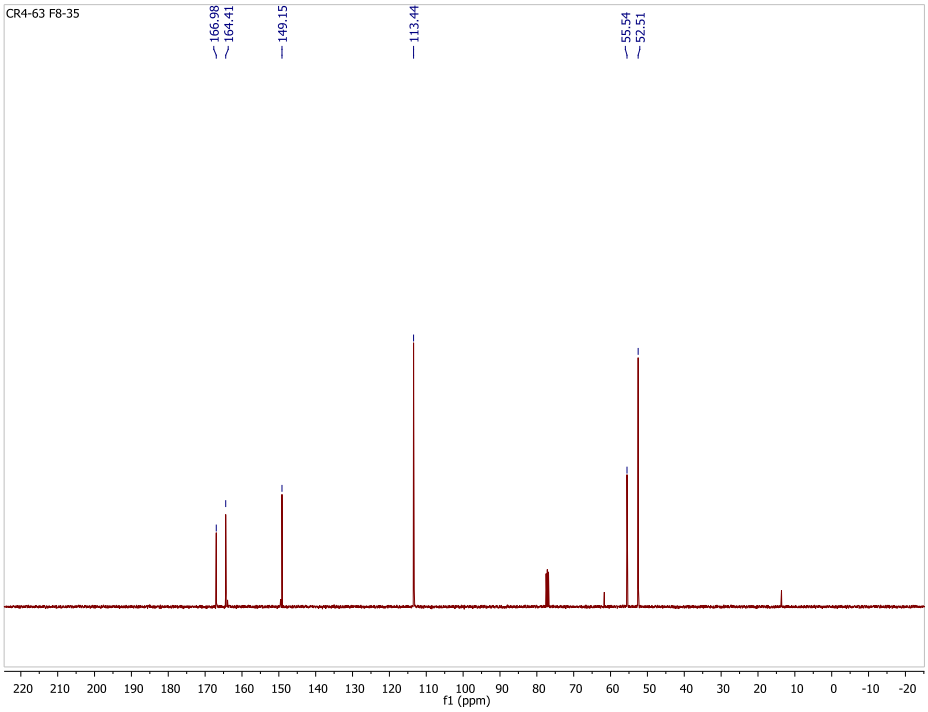

Figure S6. ^{13}C NMR of spectrum of dimethyl 4-methoxypyridine-2,6-dicarboxylate (**8**) in $CDCl_3$ (101 MHz).

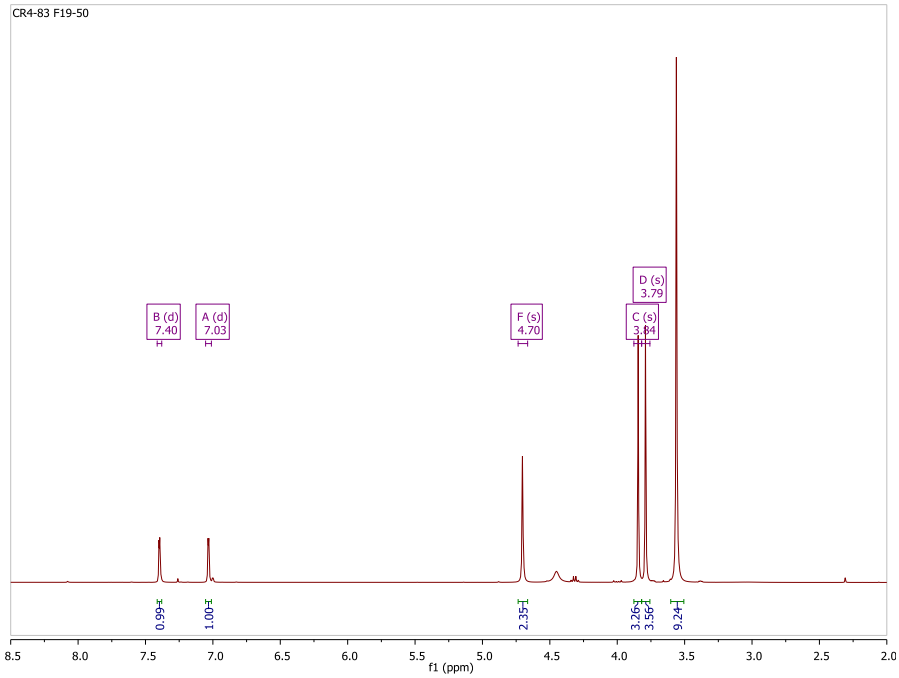

Figure S7. ^{1}H NMR of spectrum of methyl 6-(hydroxymethyl)-4-methoxypicolinate (**9**) in $CDCl_3$ (400 MHz).

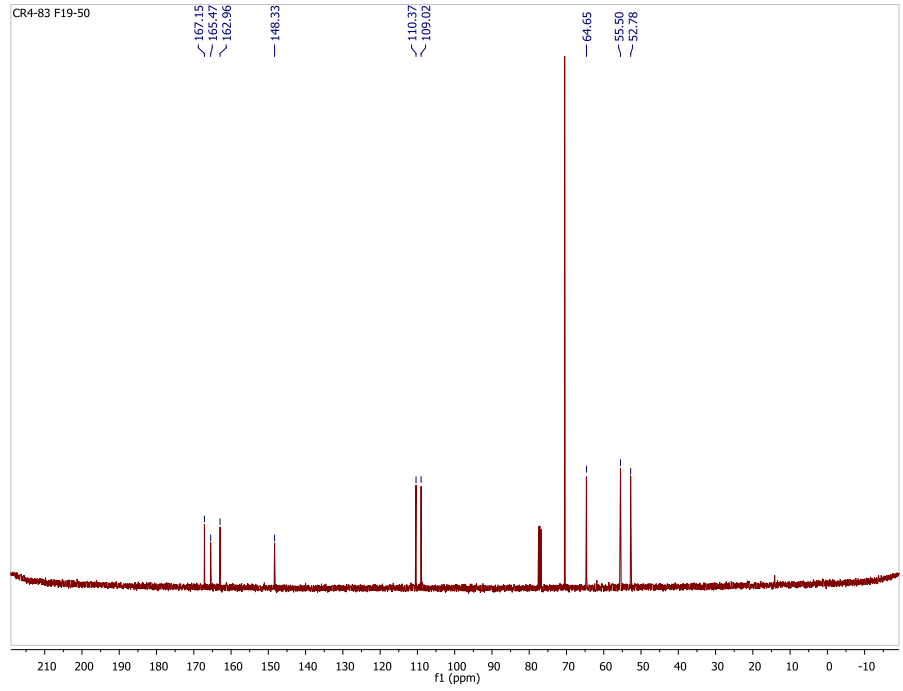

Figure S8. ^{13}C NMR of spectrum of methyl 6-(hydroxymethyl)-4-methoxypicolinate (**9**) in $CDCl_3$ (101 MHz).

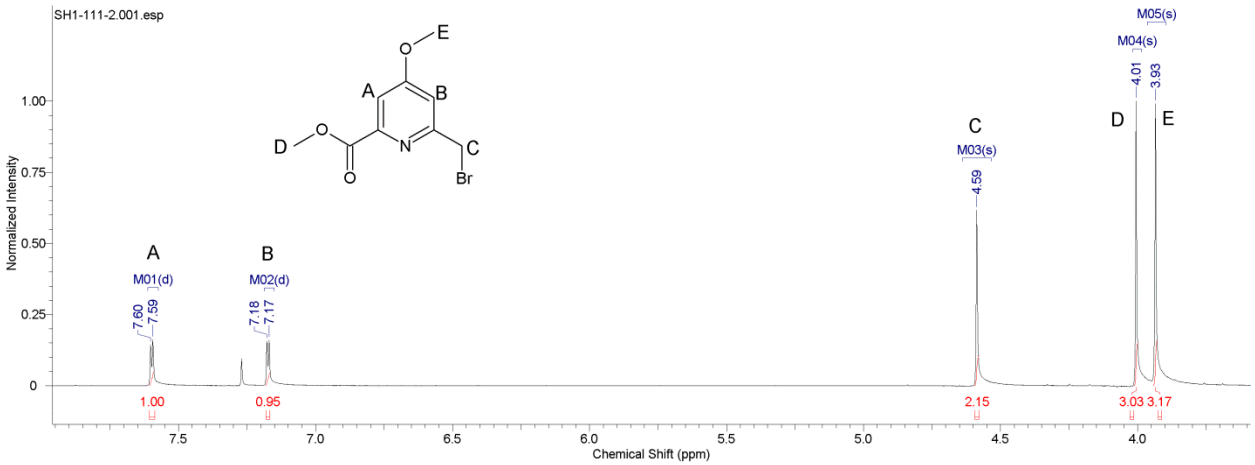

Figure S9. ^{1}H NMR of spectrum of methyl 6-(bromomethyl)-4-methoxypicolinate (**10**) in $CDCl_3$ (300 MHz).

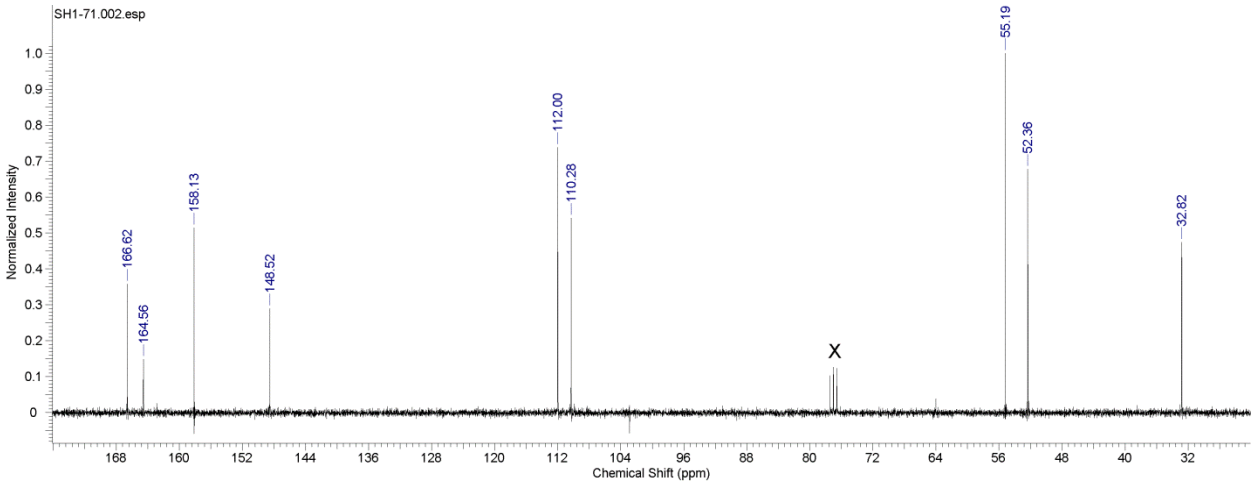

Figure S10. ^{13}C NMR of spectrum of methyl 6-(bromomethyl)-4-methoxypicolinate (**10**) in $CDCl_3$ (75 MHz).

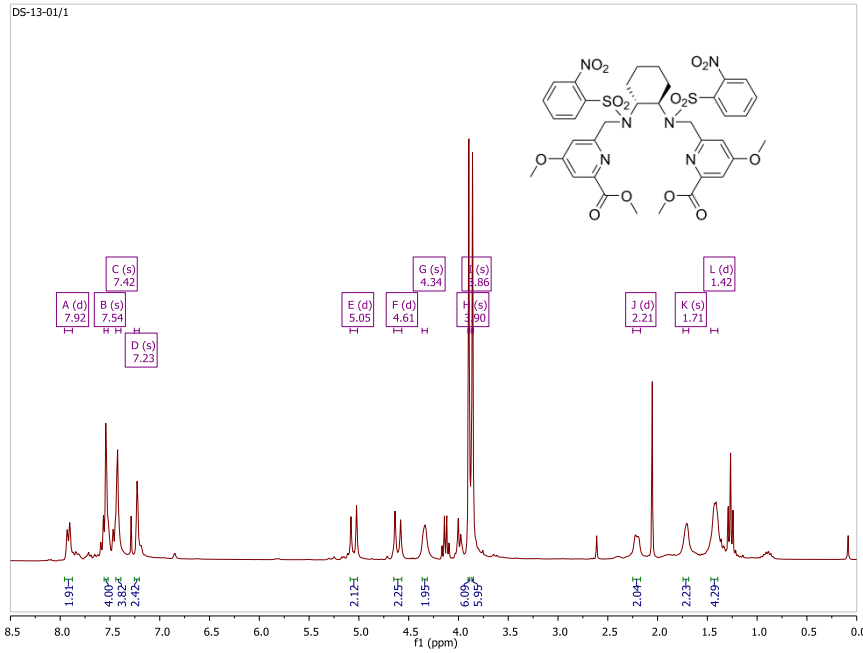

Figure S11. ^{1}H NMR of spectrum of dimethyl 6,6'-((((1*R*,2*R*)-cyclohexane-1,2-diyl)bis(((2-nitrophenyl)sulfonyl) azanediyl))bis(methylene))bis(4-methoxypicolinate) (**11**) in $CDCl_3$ (300 MHz).

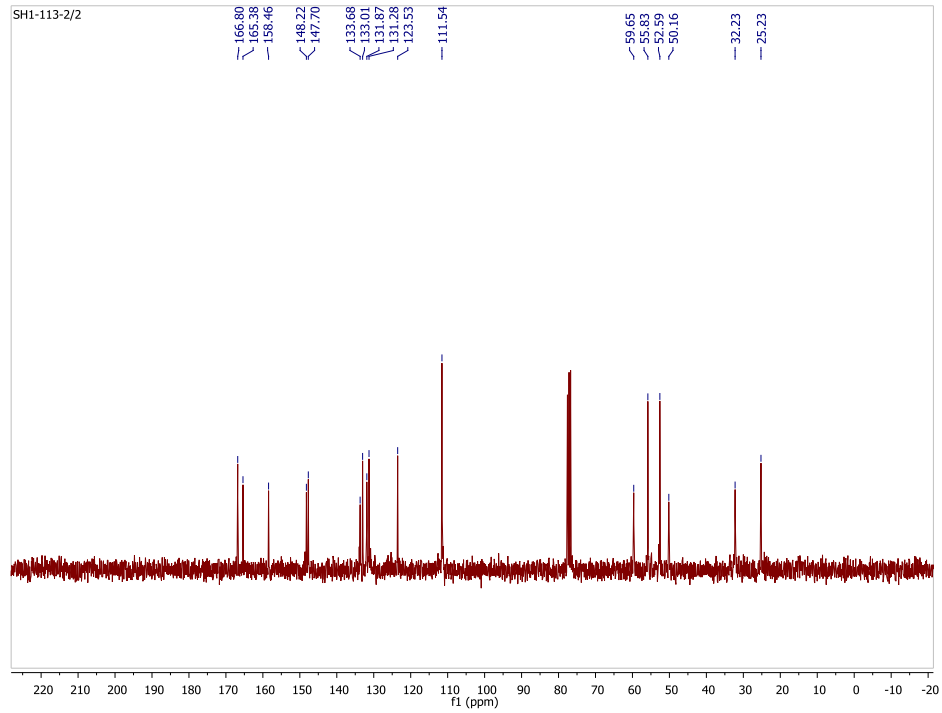

Figure S12. ^{13}C NMR of spectrum of dimethyl 6,6'-((((1*R*,2*R*)-cyclohexane-1,2-diyl)bis(((2-nitrophenyl)sulfonyl) azanediyl))bis(methylene))bis(4-methoxypicolinate) (**11**) in $CDCl_3$ (75 MHz).

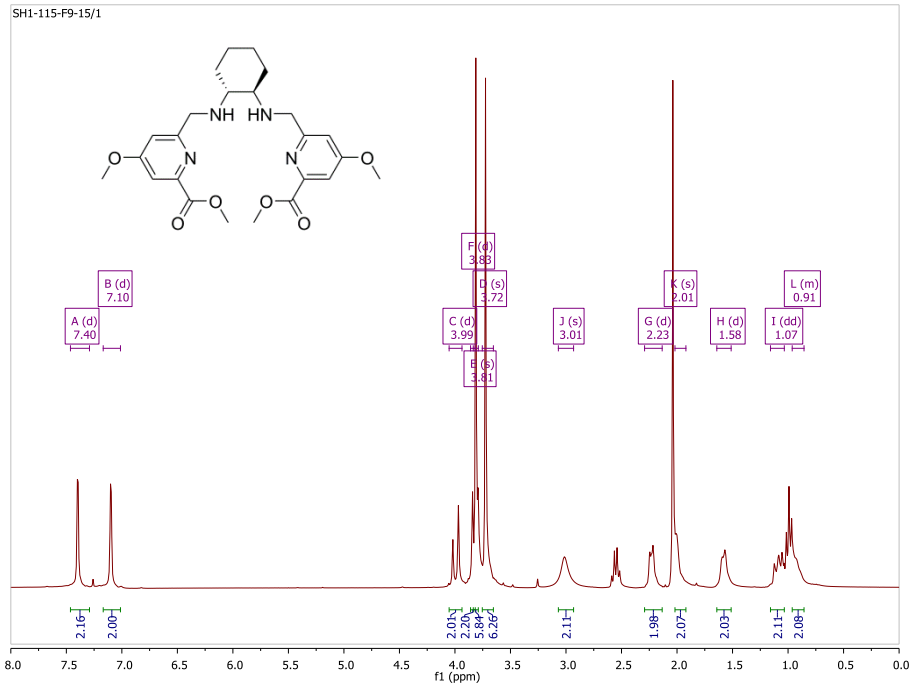

Figure S13. ^{1}H NMR of dimethyl 6,6'-((((1*R*,2*R*)-cyclohexane-1,2-diyl)bis(azanediyl))bis(methylene))bis(4-methoxypicolinate) (**12**) in $CDCl_3$ (300 MHz).

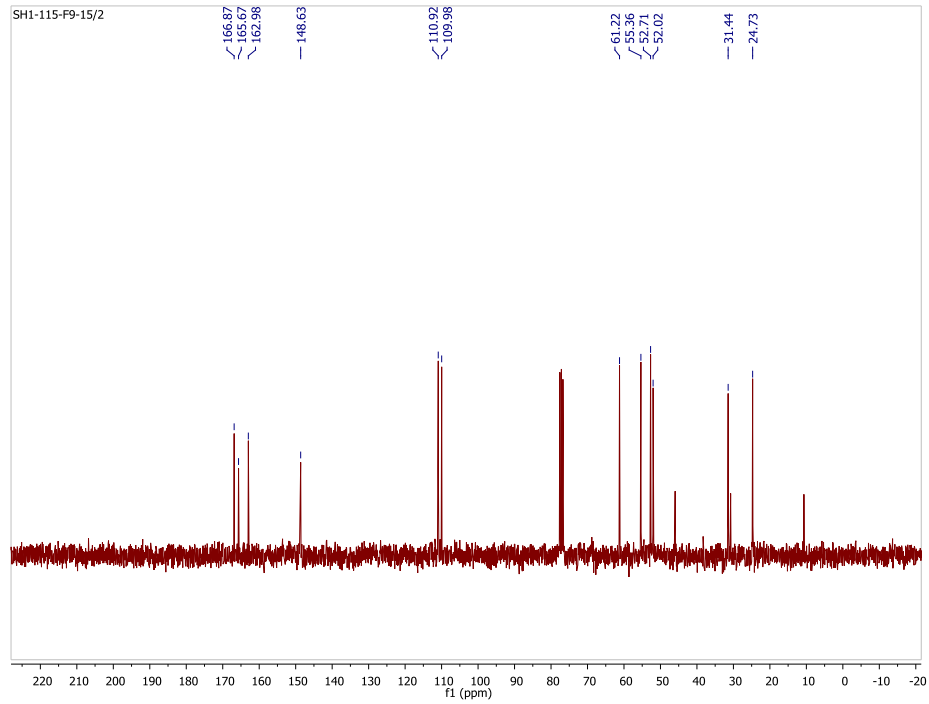

Figure S14. ^{13}C NMR of dimethyl 6,6'-((((1*R*,2*R*)-cyclohexane-1,2-diyl)bis(azanediyl))bis(methylene))bis(4-methoxypicolinate) (**12**) in $CDCl_3$ (75 MHz).

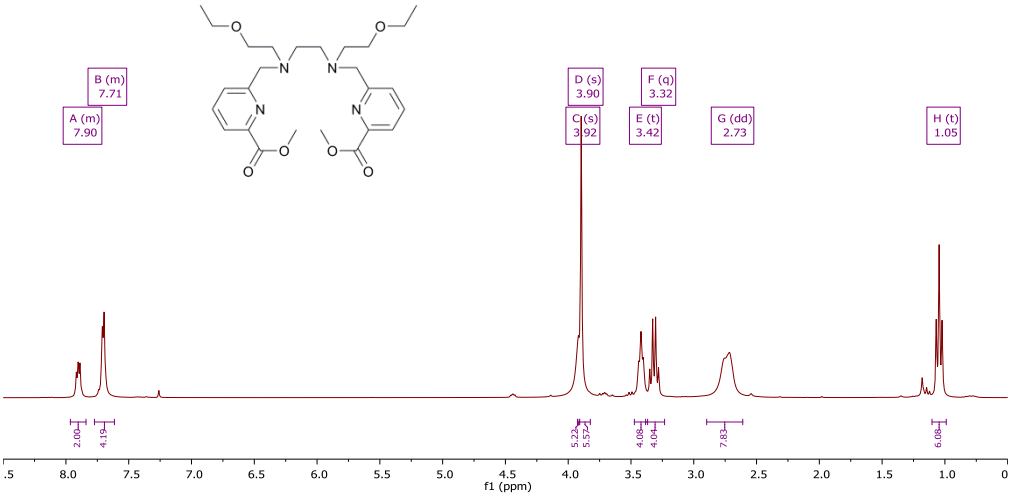

Figure S15. ^{1}H NMR of Me_2dedpa-*N,N'*-ee (**13**) in $CDCl_3$ (300 MHz).

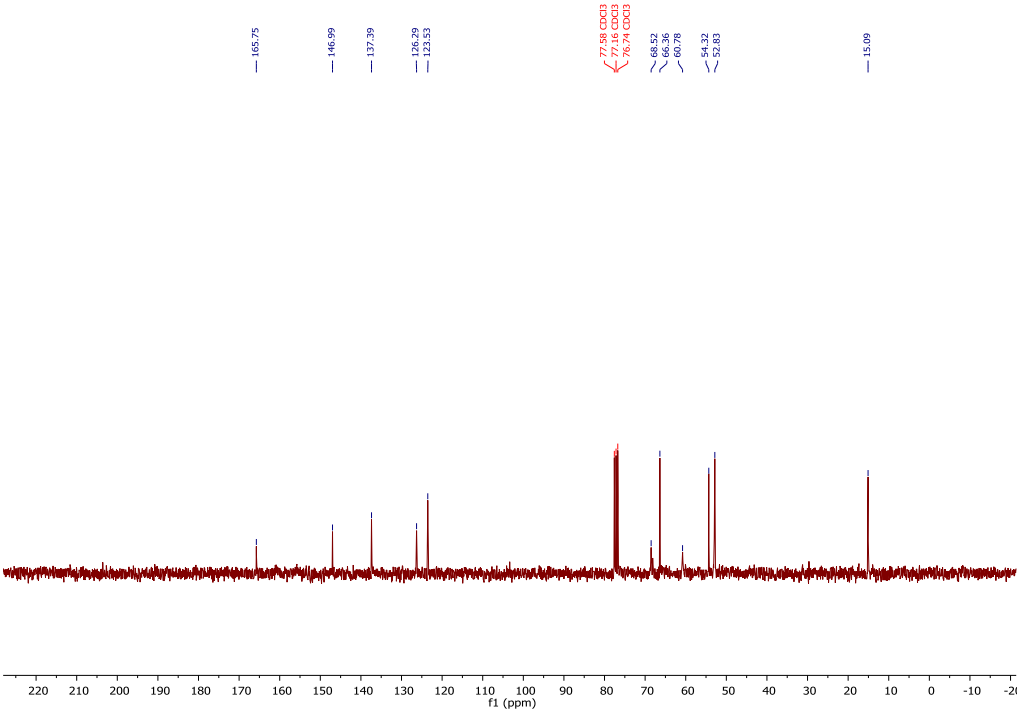

Figure S16. ^{13}C NMR of Me_2dedpa-*N,N'*-ee (**13**) in $CDCl_3$ (75 MHz).

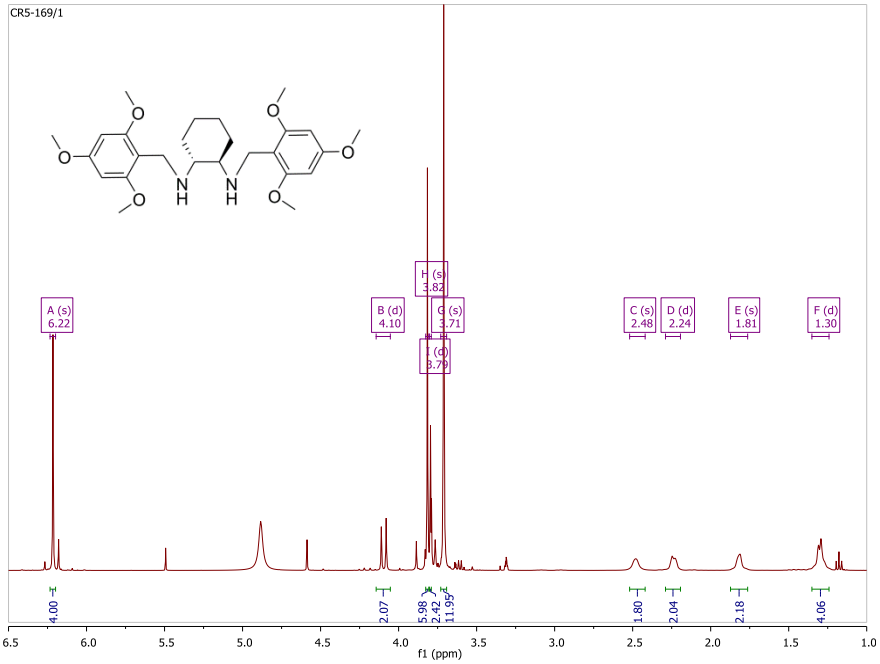

Figure S17. ^{1}H NMR of (1*R*,2*R*)-N^1,N^2-bis(2,4,6-trimethoxybenzyl)cyclohexane-1,2-diamine (**18**) in MeOD-d_4 (400 MHz).

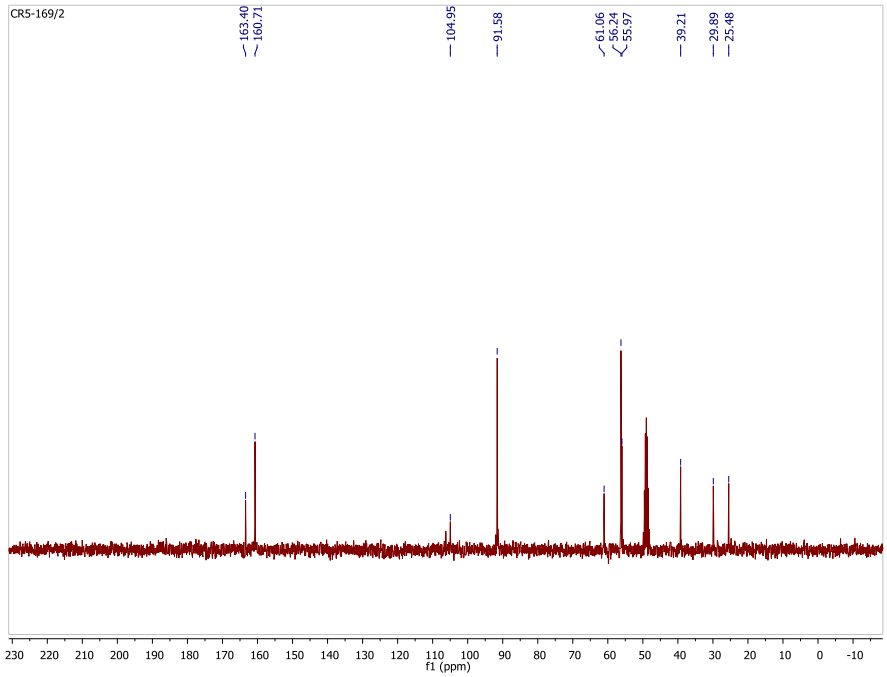

Figure S18. ^{13}C NMR of (1*R*,2*R*)-N^1,N^2-bis(2,4,6-trimethoxybenzyl)cyclohexane-1,2-diamine (**18**) in MeOD-d_4 (75 MHz).

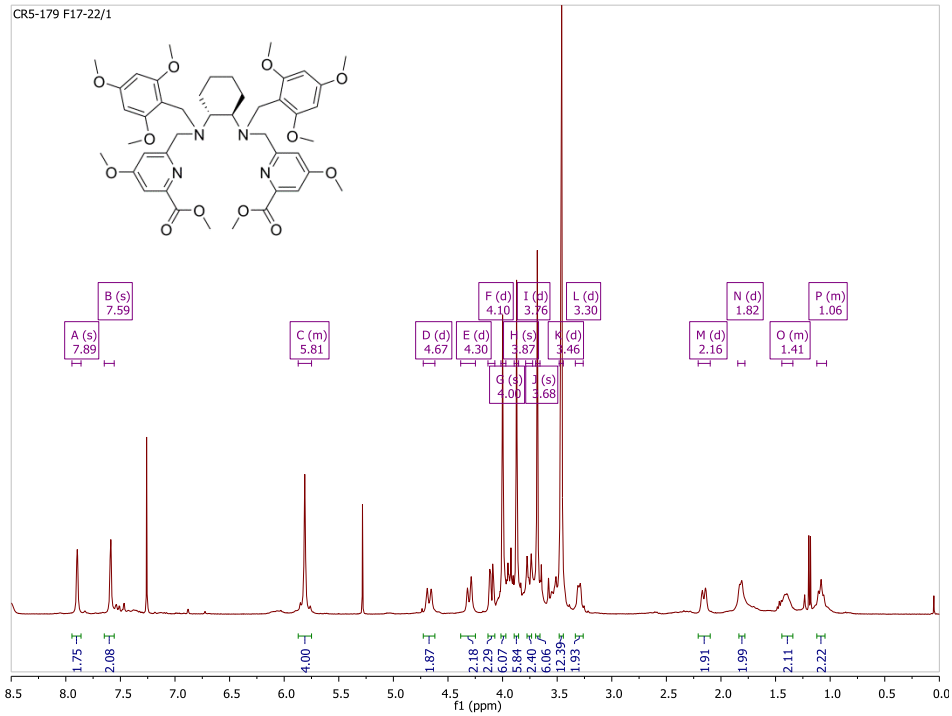

Figure S19. ^{1}H NMR of Me$_2$*CHX*dedpa$_{OMe}$-*N,N'*-Bn$_{3OMe}$ (**19**) in $CDCl_3$ (400 MHz).

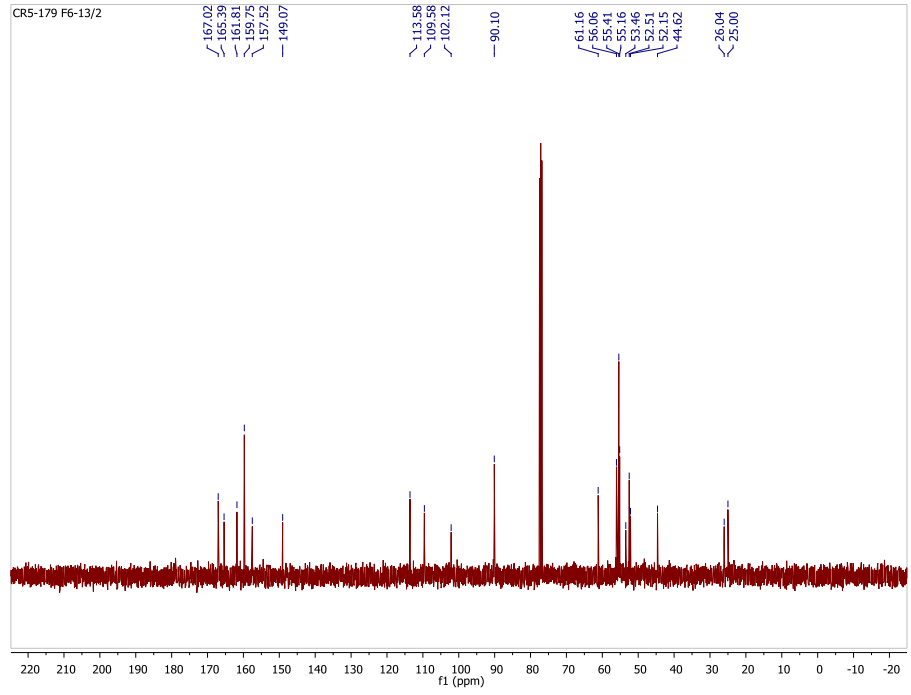

Figure S20. ^{13}C NMR of Me$_2$*CHX*dedpa$_{OMe}$-*N,N'*-Bn$_{3OMe}$ (**19**) in $CDCl_3$ (101 MHz).

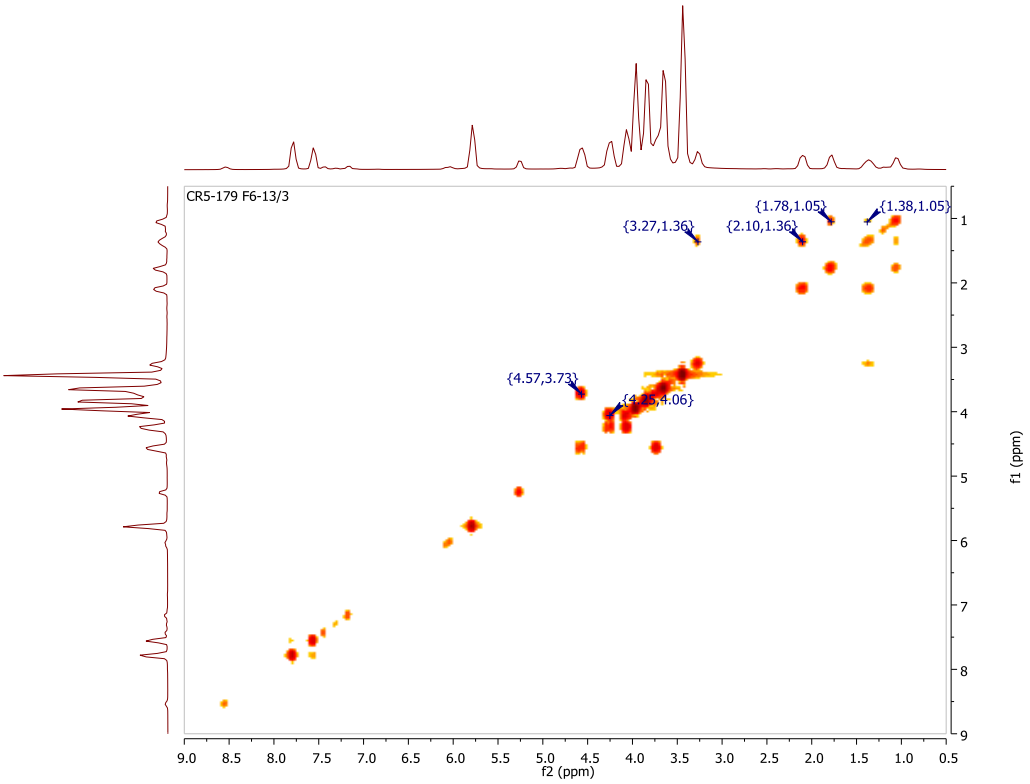

Figure S21. ^{1}H-^{1}H COSY NMR of Me_2*CHX*dedpa$_{OMe}$-*N,N'*-Bn_{3OMe} (**19**) in $CDCl_3$ (400 MHz).

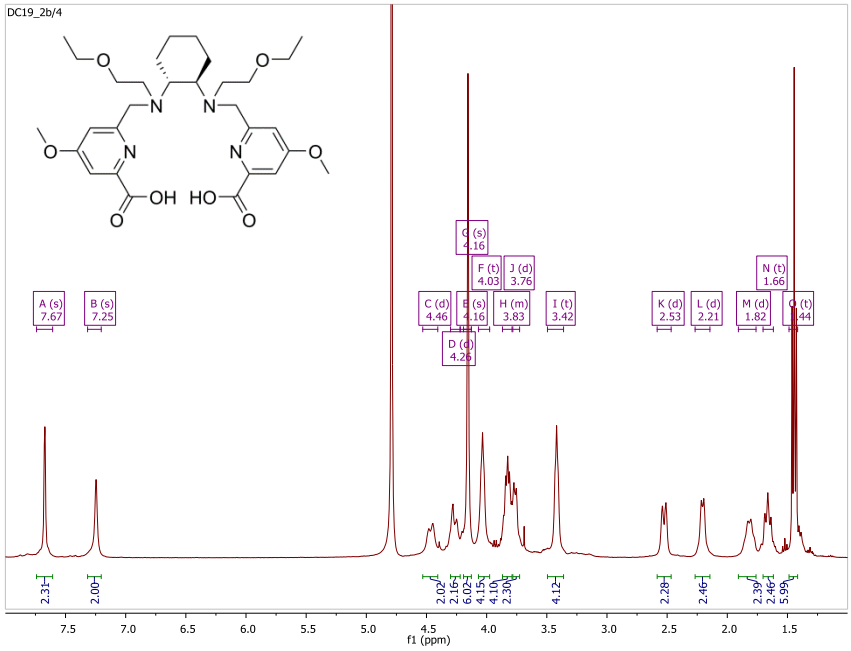

Figure S22. ^{1}H NMR of H_2*CHX*dedpa$_{OMe}$-*N,N'*-ee (**3**) in D_2O (400 MHz, 55°C).

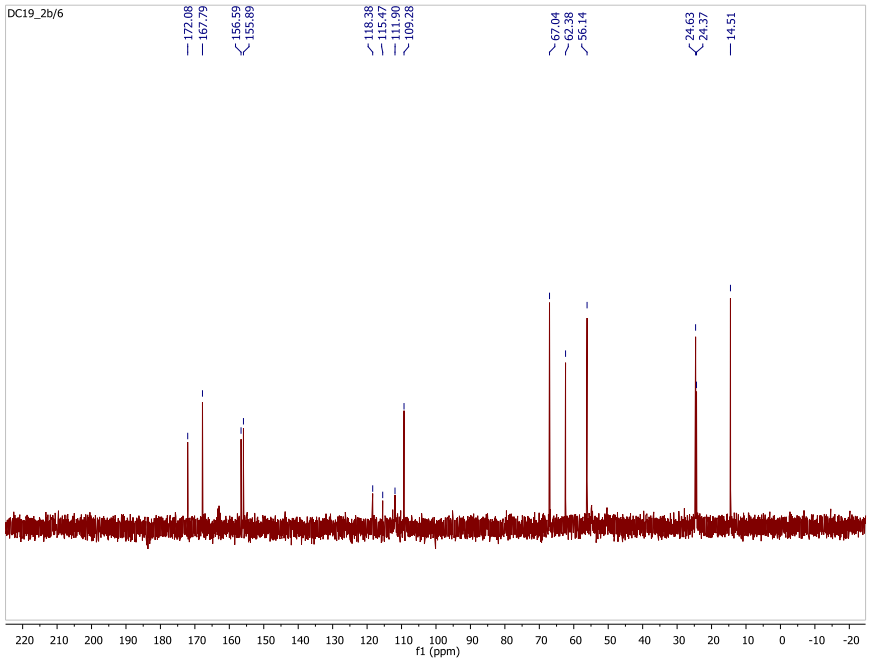

Figure S23. ^{13}C NMR of H_2*CHX*dedpa$_{OMe}$-*N,N'*-ee (**3**) in D_2O (101 MHz, 55°C).

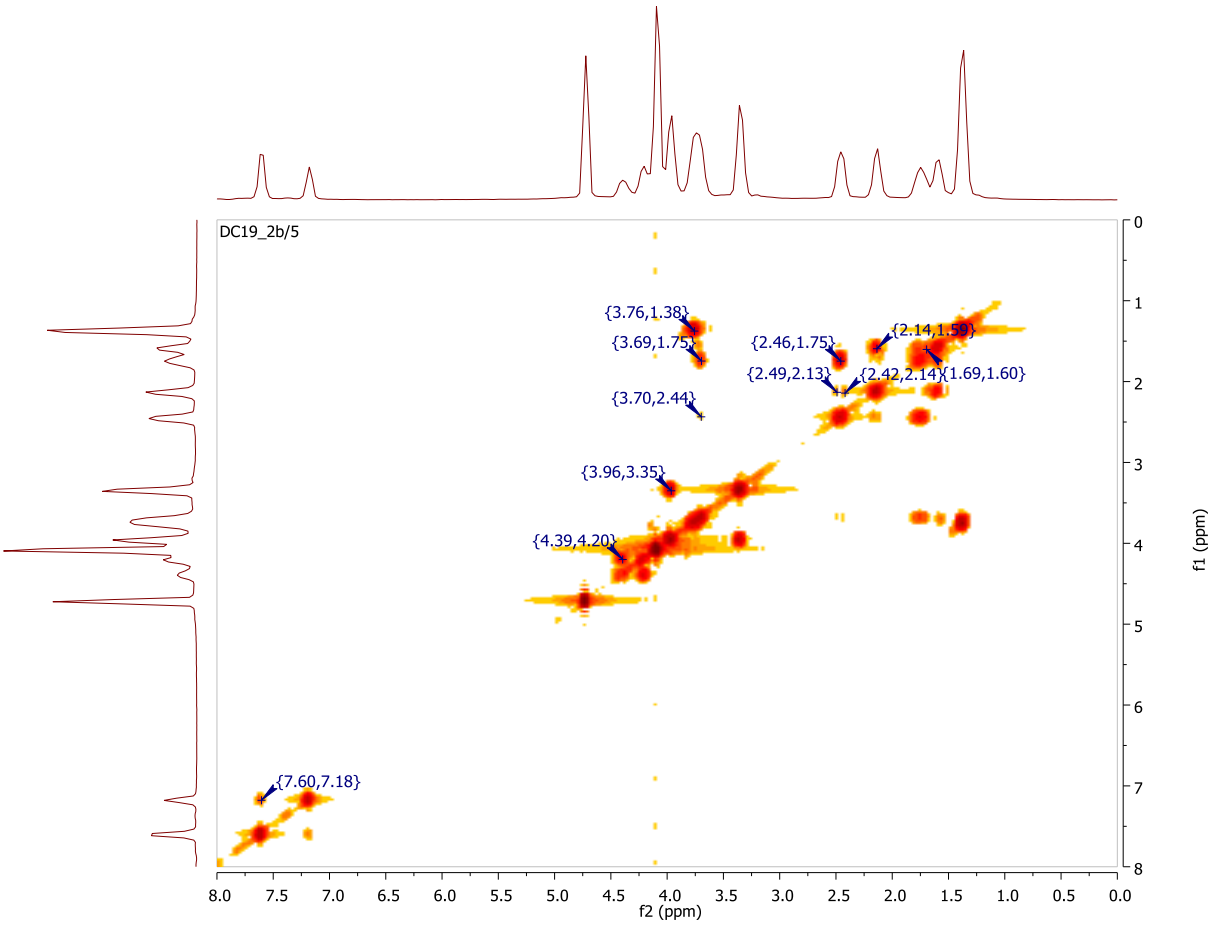

Figure S24. ^{1}H-^{1}H COSY NMR of H_2*CHX*dedpa$_{OMe}$-*N,N'*-ee (**3**) in D_2O (400 MHz, 55°C).

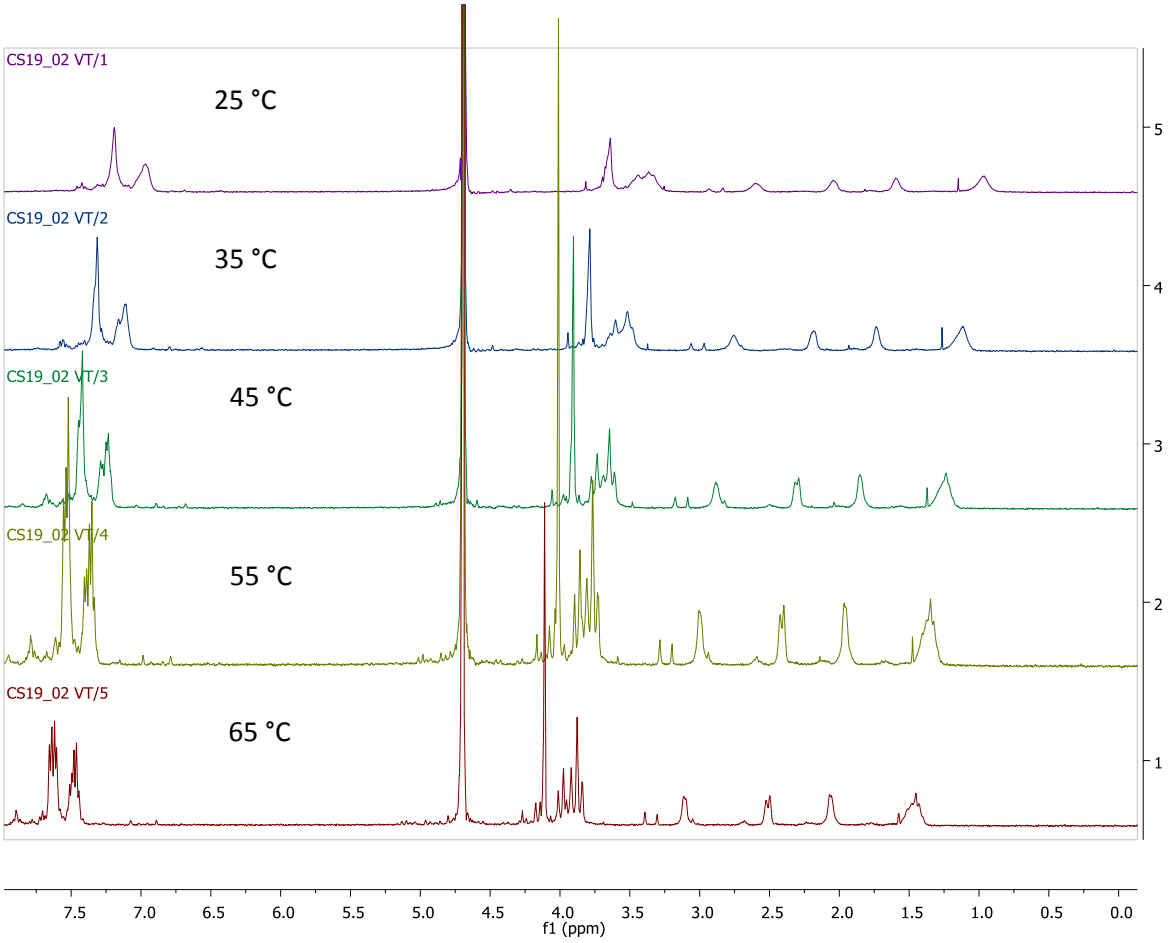

Figure S25. ^{1}H VT NMR of H_2*CHX*dedpa$_{OMe}$-*N,N'*-Bn (**4**) in D_2O (400 MHz, 25-65°C).

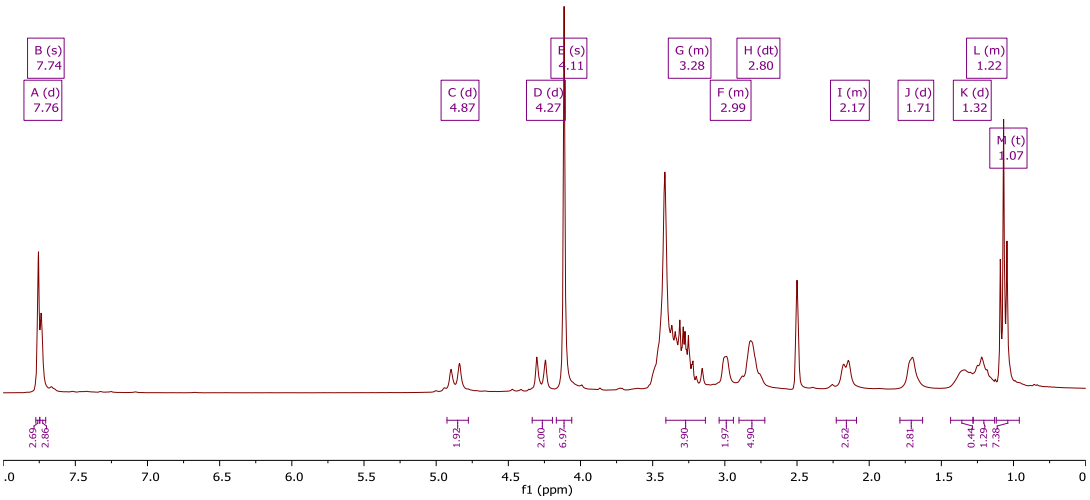

Figure S26. ^{1}H NMR of[Ga(**3**)][ClO_4] in DMSO-d_6 (300 MHz).

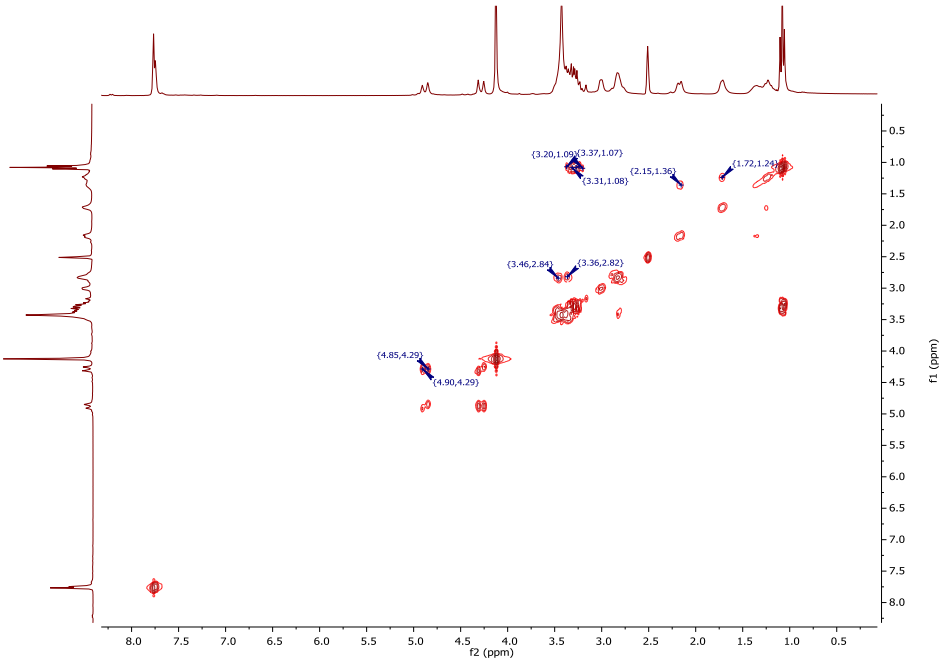

Figure S27. ^{1}H-^{1}H COSY NMR of[Ga(**3**)][ClO_4] in DMSO-d_6 (300 MHz).

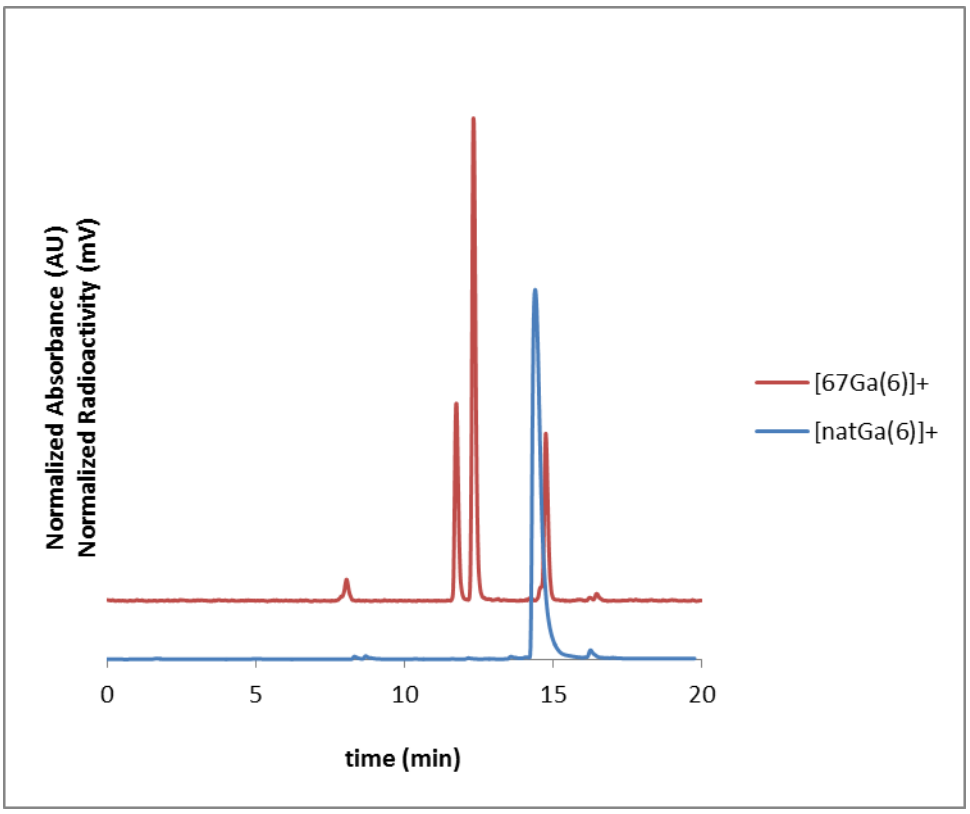

Figure S28. Stacked HPLC chromatograms of $[^{67}Ga(\mathbf{6})]^+$ (red, radiotrace; t_R = 14.57 min) and $[^{nat}Ga(\mathbf{6})]^+$ (blue, absorbance; t_R = 14.38). Small shift in retention times are due to UV-Vis and radiation detector being placed in sequence in the HPLC set-up.

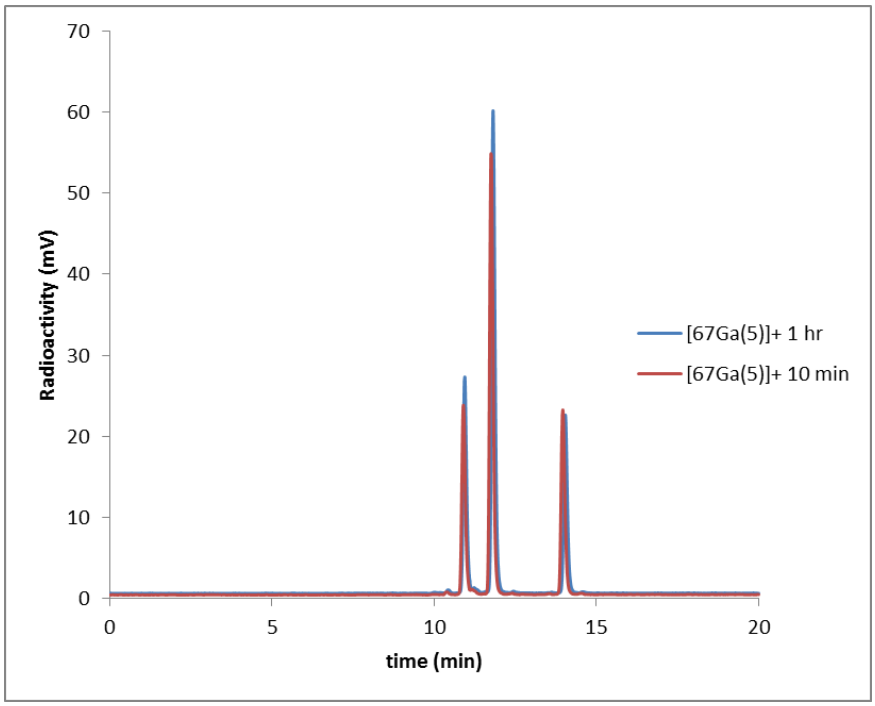

Figure S29. Overlaid HPLC radio-chromatograms of $[^{67}Ga(\mathbf{5})]^{+}$, injected at 10min and 1 hour showing no significant change in peak areas.

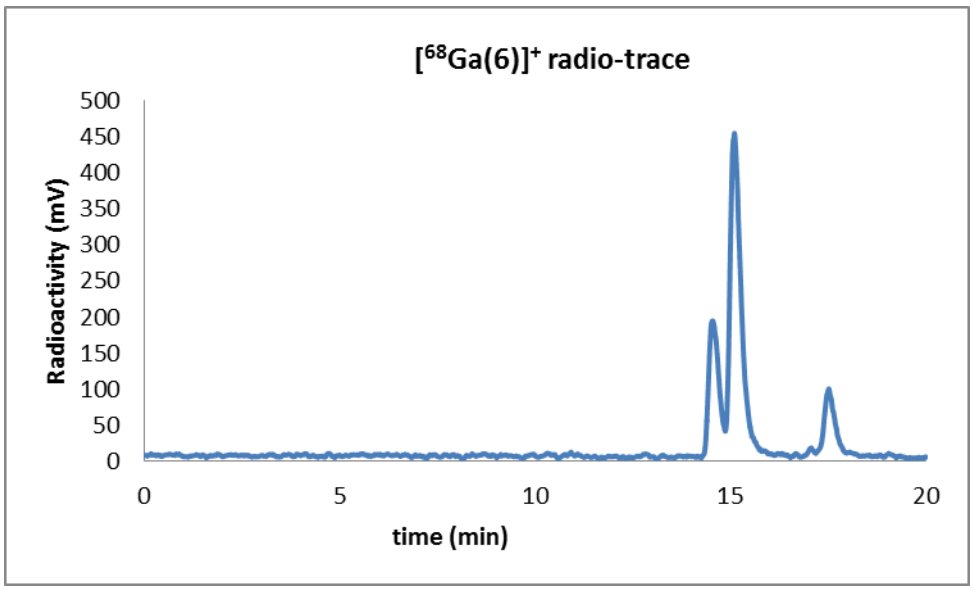

Figure S30. HPLC radio-chromatogram of [^{68}Ga(**6**)]$^{+}$, labelled at 10^{-4} M, 10 minutes at room temperature. Note: The ^{68}Ga radiolabeling experiments were analysed on a different HPLC system than the ^{67}Ga experiments, which explains the slight shift in retention times of the three product peaks compared to the [^{67}Ga(**6**)]$^{+}$ radio-trace.